

Thermally conductive phase-change materials for energy storage based on low-density polyethylene, soft Fischer-Tropsch wax and graphite

W. Mhike¹, W.W. Focke¹, J.P. Mofokeng² and A.S. Luyt^{2*}

¹ Institute for Applied Materials, University of Pretoria, Pretoria, 0002, SOUTH AFRICA

² Department of Chemistry, University of the Free State (Qwaqwa Campus), Private Bag X13, Phuthaditjhaba, 9866, SOUTH AFRICA

Abstract

Phase change materials based on graphite-filled wax/polyethylene blends could find application as thermal energy storage materials. Such compounds, comprising wax to polyethylene in a 3:2 proportion, were prepared by twin screw compounding. Two types of graphite were used in an attempt to improve the thermal conductivity of the compounds. Expanded graphite enhanced the thermal conductivity by more than 200% at a loading of 10 wt.%, compared to a ca. 60% improvement with natural graphite flakes at the same loading. The TGA results showed that all the compounds underwent a two-step degradation. In all cases the mass % ratios of the two degradation steps were roughly 3:2 for wax:LDPE, which confirms that the wax evaporated completely before the degradation of LDPE started. The DSC results suggest that the heat energy storing capacity of the wax is not influenced by the other components as long as heating is restricted to temperatures just above the melting point of the wax. It is also apparent that the presence of both forms of graphite enhanced the rate of heat transfer to the PCMs. The DMA results show that the presence of wax had a softening effect, while the presence of graphite opposed this softening effect by reinforcing the PCM composites.

Keywords: phase-change material; LDPE; paraffin wax; thermal properties; thermomechanical properties; thermal conductivity; expanded graphite

* Corresponding author (LuytAS@qwa.ufs.ac.za)

1. Introduction

Phase change materials (PCM) have been investigated for many applications, including energy storage materials, thermal protection systems, as well as in active and passive cooling of electronic devices [1,2]. Different inorganic as well as organic substances have already been used for the creation of phase change materials; among the most common ones are various salts and their eutectics, fatty acids and n-alkanes [3]. Paraffin waxes can be good phase-change materials because of their desirable characteristics such as a high latent heat of fusion, negligible super-cooling, low vapour pressure in the melt, chemical inertness and stability [4]. The number of carbon atoms in the chains of paraffin waxes with melting temperatures between 30 °C and 90 °C ranges from 18 to 50 (C18–C50). The specific heat capacity of latent heat paraffin waxes is about 2.1 J g⁻¹ K⁻¹. Their melting enthalpy lies between 180 and 230 J g⁻¹, which is quite high for organic materials. The combination of these two values results in an excellent energy storage density. Waxes are also readily available and inexpensive [5,6].

Traditionally, paraffin waxes are kept in closed tanks or containers during heating to suppress wax leakage. Another possibility to keep waxes in a stable shape during application is to blend them with convenient polymers. The polymer matrix fixes the paraffin wax in a compact form, even after melting, and suppresses wax leakage. Such materials are also easily shaped, and the polymer phase provides its own specific properties. Polyethylene seems to be the most frequently used polymer for blending with paraffin waxes to obtain shape stabilized PCM [4,7]. For example, Inaba and Tu [7] investigated a shape-stabilized paraffin wax system based on paraffin wax blended with high-density polyethylene (HDPE), while Krupa *et al.* [8] investigated the thermal and thermo-mechanical properties of shape stabilized phase change materials based on low density polyethylene and Fischer-Tropsch paraffin waxes. They found that, although LDPE still formed the continuous phase up to 50 wt.% wax, the amount of LDPE at such a high wax content is not enough to keep the material structure in a consistent shape.

One problem with shape-stabilized phase-change materials based on wax and polyethylene is, however, that both components are poor heat conductors with the result that heat transport to and from the phase-change material is relatively slow. Several authors investigated the improvement of heat conduction by the addition of conductive filler into the phase-change material. Some of them [9,10] investigated the dispersion of exfoliated graphite

nanoparticles in liquid paraffin, and its influence on the thermal conductivity and heat storage capacity of the phase-change material. They found an improvement in thermal conductivity without reducing the heat storage capacity of the paraffin. Fukai *et al.* [11] did a similar investigation using carbon fibre brushes in n-octadecane, and Cui *et al.* [12] on carbon nanofibres and carbon nanotubes in soy wax and paraffin wax. Xiang and Drzal, in their investigation of exfoliated nanoplatelets in paraffin wax, found that higher thermal conductivity of the composite PCM can be achieved with nanofillers with larger aspect ratio, better orientation and lower interface density [13]. Xia *et al.* [14] also investigated expanded graphite (EG)/paraffin composite PCMs. They found that EG networks, that formed with increasing mass fraction of EG, provided thermal conduction paths which enhanced the thermal conductivity of the PCMs.

There are very few reports on the improvement of the thermal conductivity of polyethylene/PCM blend materials. Molefi *et al.* [15-17] investigated the morphology, thermal and thermomechanical properties, as well as the thermal conductivities, of different polyethylenes mixed with different amounts of Fischer-Tropsch paraffin wax, as well as different amounts of copper micro- and nanoparticles. They found that the presence of the wax had the biggest influence on the mechanical properties of the phase-change composites, and that the wax preferably crystallized around the copper particles. The presence of copper particles observably improved the thermal conductivities of the samples. However, in these investigations the wax contents were too low for the samples to be effective phase-change materials.

This paper reports on the successful melt-blending of wax and LDPE, at a high wax:LDPE mass ratio of 3:2, with different amounts of normal and exfoliated graphite. We discuss the morphology, thermal conductivity, dynamic mechanical behaviour and thermal stability of these PCM blend composites, as well as the respective influence of wax and LDPE on each other's melting and crystallization behaviour and the influence of graphite on this behaviour.

2. Experimental

2.1 Materials

The wax used was EXP 1644, an experimental Fischer-Tropsch wax from Sasol Wax. It was specifically designed for energy storage applications. The low-density polyethylene (LDPE) was injection moulding grade LT019 from Sasol Polymers (density 0.919 g cm^{-3} ; MFI $20.5 \text{ g} / 10 \text{ min} @ 190 \text{ }^\circ\text{C} / 2.16 \text{ kg}$). Zimbabwean flake graphite (referred to as ‘graphite’ in the rest of the paper) with a particle size distribution shown in Figure 1 and a d_{50} particle size of $117.8 \text{ }\mu\text{m}$ (Mastersizer Hydrosizer 2000, Malvern Instruments, Malvern, UK) was supplied by BEP Bestobell, Johannesburg. Expandable graphite ES 250 B5 with a particle size distribution shown in Figure 1 and a d_{50} particle size of $381.2 \text{ }\mu\text{m}$ was supplied by Qingdao Kropfmuehl Graphite (Hauzenberg, Germany). The graphite specific surface areas were obtained using a Nova 1000e BET in N_2 at 77 K and are given in Table 1.

2.2 Formulation

The wax:polyethylene mass ratio was maintained at 3:2 throughout. Table 2 shows the amounts of materials used in the composites.

2.3 Mixing, compounding and hot pressing

2.3.1 Mixing

Wax/LDPE

LDPE powder (300 g) was weighed and spread evenly into a silicone baking pan. The powder was more or less evenly covered with lumps of wax (450 g). The sample was placed in a preheated oven at $130 \text{ }^\circ\text{C}$ and allowed to melt. After melting the blend was allowed to cool to room temperature whilst being stirred until solidification. The cake was granulated before being compounded.

Wax/LDPE/graphite

The relevant quantities of Zimbabwean graphite and LDPE as indicated in Table 2 were measured and manually mixed together with a spatula. Lumps of wax (450 g) were then spread on top of the mix. The composition was put into a preheated oven at $130 \text{ }^\circ\text{C}$ and

allowed to melt. After melting the composite was allowed to cool to room temperature whilst being stirred until solidification. The cake was granulated before being compounded.

Wax/LDPE/e-graphite

The expandable graphite was heated in a furnace to 600 °C using a steel container and maintained at that temperature for 10 minutes to form expanded graphite (referred to as 'e-graphite' in the rest of the paper). It was then poured into a silicon baking pan and mixed with LDPE, before the lumps of wax were spread on top of the composition. Table 2 shows the quantities used. The composition was put into a preheated oven at 130 °C and allowed to melt. After melting the composite was allowed to cool to room temperature whilst being stirred until solidification. The cake was granulated before being compounded.

2.3.2 Compounding

Compounding was carried out in a TX28P laboratory scale co-rotating 28 mm twin screw extruder with an L/D ratio of 18. The temperature profile is shown in Table 3. The extrudate was collected in a water bath at room temperature, after which it was dried in ambient conditions for five days.

2.3.3 Hot pressing

Sheets were pressed in a Vertex heated hot press. The extrudate was first compacted at 19.5 MPa for one minute to remove entrapped air. They were then hot pressed at 140 °C for 10 minutes at 19.5 MPa and allowed to cool slowly to room temperature while maintaining the applied pressure.

2.4 Analyses

2.4.1 Scanning electron microscopy (SEM)

The graphite structures shown in Figure 2 were observed using JEOL JSM 5800LV (low resolution micrographs) and a Zeiss Ultra FESEM (high resolution micrograph) scanning

electron microscopes. The graphite particles were stuck on double sided tape which was affixed on a metal plate. Accelerating voltages of 20 kV and 1 kV were used for the analysis using the JEOL JSM 5800LV and Zeiss Ultra FESEM respectively, with no electroconductive coating on the graphite particles, since they were conductive.

The graphite dispersion in the wax/polyethylene blend was observed using a Tescan VEGA3 scanning electron microscope. The uncoated surfaces of the melt pressed samples were analysed at an accelerating voltage of 30 kV and 200x magnification.

2.4.2 Thermal conductivity

Thermal conductivity measurements were performed on 3 mm thick sample discs 60 mm in diameter using a ThermTest Inc. Hot Disk® TPS 500 Thermal Constants Analyser. The instrument uses the transient plane source method. A 6.403 mm Kapton disk type sensor was selected for the analysis. The sensor was sandwiched between two sample discs. A linear low-density polyethylene disc was inserted in-between the sample and the sample holder on both sides of the sample in order to reduce heat loss. Three measurements were performed for each composition.

2.4.3 Thermogravimetric analysis (TGA)

Samples of mass 5-10 mg were heated at $10\text{ }^{\circ}\text{C min}^{-1}$ from ambient to $600\text{ }^{\circ}\text{C}$ under nitrogen flow (20 mL min^{-1}) in a Perkin Elmer TGA7 ((Waltham, Massachusetts, USA).

2.4.4 Differential scanning calorimetry (DSC)

All the composites were analysed in a Perkin Elmer Pyris 1 differential scanning calorimeter (Waltham, Massachusetts, USA) under the following conditions: (1) One sample was heated at $10\text{ }^{\circ}\text{C min}^{-1}$ from 0 to $70\text{ }^{\circ}\text{C}$ (just above the wax melting range), cooled at the same rate to $0\text{ }^{\circ}\text{C}$, and re-heated at the same rate to $150\text{ }^{\circ}\text{C}$; (2) A second sample was heated at $10\text{ }^{\circ}\text{C min}^{-1}$ from 0 to $150\text{ }^{\circ}\text{C}$, cooled at the same rate to $0\text{ }^{\circ}\text{C}$, and re-heated at the same rate to $150\text{ }^{\circ}\text{C}$.

In a second set of experiments the samples were heated at $200\text{ }^{\circ}\text{C min}^{-1}$ from ambient to $45\text{ }^{\circ}\text{C}$, and kept isothermal at this temperature for 10 min. All the DSC experiments were

performed under a 20 mL min^{-1} nitrogen flow, and the sample masses were between 5 and 10 mg. The DSC curves were normalised with respect to the sample mass.

2.4.5 Dynamic mechanical analysis (DMA)

The dynamic mechanical analyses were performed in the bending mode in a Perkin Elmer Diamond DMA from -60 to $100 \text{ }^\circ\text{C}$ at $3 \text{ }^\circ\text{C min}^{-1}$. The initial force was 2 N and the analysis frequency was 1 Hz.

3. Results and discussion

3.1 Thermal conductivity

From Figure 3 it is evident that the thermal conductivity of the composites increased with increasing graphite content, with the increase being more significant for the samples containing e-graphite. An increase of more than 200% in the thermal conductivity was observed at 10 wt.% loading of the e-graphite, while only a 60% increase was observed for the composite with the natural graphite at the same loading. The increase in conductivity in both cases followed an almost linear trend. The reason for this difference in thermal conductivity is clear from the SEM pictures in Figure 4, which presents the images of two samples that respectively contained the same amounts of graphite and e-graphite. Compared to the graphite containing sample (Figure 4a), the e-graphite containing sample (Figure 4b) clearly shows a much better dispersion of smaller graphite particles (black), with smaller LDPE/wax areas (white) between these particles, and more well-defined thermal conductive networks, as was also observed by Xia *et al.* [14].

It is well known that large amounts of inorganic filler may reduce the mechanical properties of polyolefins and make them more brittle. This is especially true when the polymer is blended with a large amount of paraffin wax and graphite particles that act as stress concentration points in the amorphous parts of the polymer. It is therefore beneficial if the thermal conductivity can be increased so significantly with only small amounts of graphite particles dispersed in the wax/LDPE matrix. The improved thermal conductivity in the presence of these particles also means that heat may be transferred faster between the wax phase-change material and the environment around the wax/LDPE composite.

3.2 Thermogravimetric analysis (TGA)

The TGA curves of all the samples are shown in Figures 5 and 6. It is clear that the wax is much less thermally stable than the LDPE, and that the different blends and composites have intermediate thermal stabilities. The wax does not decompose, but evaporates at a much lower temperature than the decomposition temperature of LDPE. As a result the wax/LDPE blend and the composites show two mass loss steps. The first step is obviously due to the evaporation of the wax, while the second step is due to the degradation of LDPE. In all the cases the mass % ratios of the two steps are roughly 3:2 for wax:LDPE, which confirms that the wax evaporated completely before the degradation of LDPE started. For all the composites there is a good correlation between the % residue at 600 °C and the amount of graphite originally mixed into the composite, which confirms that the graphite was generally well dispersed in the wax/LDPE blend.

The thermal stability of the wax/LDPE blend seems to improve in the presence of and with increasing graphite content. The most probable reason for this is that (i) the interaction between the wax or LDPE chains and the graphite particles reduces the free radical chain mobility and thus slows down the degradation process, and/or (ii) the interaction between the volatile degradation products and the graphite particles slows down the volatilization of these products.

3.3 Differential scanning calorimetry (DSC)

All the samples were heated to 70 °C, which is between the melting peaks of pure wax and pure LDPE, cooled to 0 °C, and re-heated to 150 °C. The re-heating curves are presented in Figures 7 and 8. Another set of samples were heated to 150 °C, cooled to 0 °C and re-heated to 150 °C. The re-heating curves in this case are presented in Figures 9 and 10. The idea was to compare the DSC heating results of samples having two different thermal histories. In the first case (Figures 7 and 8) only the wax in the blend and composites would have melted and re-solidified, while in the second case (Figures 9 and 10) both the wax and LDPE would have melted and re-solidified. Tables 4 and 5 show the observed melting peak temperatures and enthalpies for the wax- and LDPE melting peaks respectively. The ΔH^{calc} values are the

expected melting enthalpies for wax or LDPE based on the measured melting enthalpies for the pure components and the mass fraction of each component in the blend/composite.

In both the investigated cases it is interesting to see that there is a change in the shape of the wax melting peak for the blend and the composites (Figures 7 to 10). The pure wax has two overlapping peaks of which the first one is a solid-solid transition [18] and the second one is the melting of the wax. When mixed with LDPE, whether in the presence or absence of graphite, the wax melting peak shows a peak shoulder at the higher temperature side of the peak. It seems as if there could have been some co-crystallization of the lower molecular weight fractions of the LDPE with the wax. However, the temperature of the main melting peak did not change significantly. In the first case (Figures 7 and 8) the experimentally observed wax melting enthalpies are slightly lower than the calculated ones, which indicates good phase separation between the wax and LDPE, but also some co-crystallization of the wax with the LDPE. In the second case (Figures 9 and 10) the wax melting enthalpies show a similar trend, although the differences between the observed and calculated values are larger in this case.

The shape of the LDPE melting peak is, however, quite different for the two investigated cases. In the first case (Figures 7 and 8), where only wax (and maybe low molecular weight LDPE fractions) has melted during the first heating run, the LDPE melting peaks of the blend and composites have the same basic shape as that of pure LDPE (a 'peak' around 75 °C followed by a higher temperature peak). The peak shoulder appears at the same temperature for pure LDPE, the blend and the composites. This 'peak' is probably the result of some annealing of the LDPE that took place during the isothermal time at 70 °C after the first heating. However, the main peak is much less intense and appears at a lower temperature for the blend and the composites. The experimental melting enthalpies for LDPE in the blend and composites were observably higher than the calculated values. This confirms the co-crystallization of some of the wax with the LDPE, but could also have been the result of the annealing mentioned above. In the second case (Figures 9 and 10), where LDPE was also molten during the first heating run, the lower temperature peak shoulder is not visible for pure LDPE, the blend and the composites. The melting enthalpies in this case are much lower than the calculated values. This indicates possible co-crystallization of the lower LDPE fractions with the wax, but it could be that the presence of molten wax in some way inhibited the crystallization of the LDPE.

To summarize, it seems as if (i) the heat energy storage capacity of the wax was reduced by about 5% when blended with LDPE, as long as heating is restricted to temperatures just above the melting of the wax, and (ii) the presence, type and amount of graphite did not really influence the crystallization and melting behaviour of the wax and LDPE. In order to investigate whether the presence and type of graphite had any influence on the rate of heat transfer to the wax, an experiment was set up where the samples were heated very fast from ambient to 45 °C (which is just after the onset of melting of the wax), and kept isothermal at this temperature for 10 minutes while recording the melting endotherm of the wax. Figures 11 and 12 show the results of this experiment. Although the differences between the melting endotherms of the wax/LDPE blend and the composites containing different types and amounts of graphite are not significant (because of the very small samples used in DSC analyses), the peak maximum times for the graphite-containing samples are lower than that of the wax/LDPE blend. The melting peaks of the wax in the composites are also observably narrower than that of wax in the blend. These observations clearly indicate more effective heat transfer from the surroundings to the phase change material.

3.4 Dynamic mechanical analysis

The DMA results of all the investigated samples are reported in Table 6 and Figures 13 and 14. From the data in Table 6 it is clear that the presence of wax reduces the storage modulus of LDPE at -40 °C (below the LDPE glass transition) and at 70 °C (above the LDPE glass transition and wax melting). The decrease is quite significant above the wax melting temperature. This is to be expected, because the wax (both in its solid and liquid state) softens the wax/LDPE matrix. An increase in graphite content increases the storage modulus, and this increase is more significant for exfoliated graphite, where the E' values for the 10 wt.% sample correlates well with those of the 25 wt.% graphite containing sample. A final observation is that the samples with higher graphite contents have E' values of the same order of magnitude than those of LDPE. The presence of graphite therefore reinforces the sample and counters the softening effect of the wax.

Figures 13 and 14 show that the glass transition of LDPE seems to broaden and shift to higher temperatures for the blend and composites. The only possible explanation for this is that the wax crystals and graphite particles in the amorphous phase of the LDPE immobilize the LDPE chains and as a result shifts the glass transition to higher temperatures. In all the

blend and composite samples the wax melting can be clearly observed as a strong decrease in loss modulus above 40 °C. It does not seem as if the presence of graphite in any form or amount had a significant influence on the loss modulus behaviour of the blend.

4. Conclusions

The influence of two different kinds of graphite, normal Zimbabwean graphite and exfoliated graphite, on the thermal conductivity, thermal stability, thermomechanical behaviour, as well as melting and crystallization behaviour of a wax/LDPE blend with a high wax:LDPE ratio was investigated. The thermal conductivity of the wax/LDPE/graphite composites increased with increasing graphite content, but much better thermal conductivity was found for the samples containing exfoliated graphite, with a 200% increase in thermal conductivity for samples containing only 10 wt.% exfoliated graphite. The TGA results showed that (i) wax, LDPE and graphite were well distributed in the blend and in the different composites, and (ii) the presence of graphite slows down the degradation of the wax/LDPE blend. The melting and crystallization behaviour of the wax and LDPE strongly depended on the thermal history of the samples, but the presence, type and amount of graphite did not influence this behaviour. The DMA results confirmed the softening effect of the wax and the reinforcing effect of the graphite in the different investigated samples. Generally the thermal and thermomechanical behaviour of the PCM composites depended very little on the type of graphite used.

References

1. B. Zalba, J.M. Marin, L.F. Cabeza, H. Mehling, Review on thermal energy storage with phase change: materials, heat transfer analysis and applications, *Applied Thermal Engineering* 23 (2003) 251–283.
2. A.M. Khudhair, M.M. Farid, A review on energy conservation in building applications with thermal storage by latent heat using phase change materials, *Energy Conversion and Management* 45 (2004) 263–275.
3. M. Kenisarin, K. Mahkamov, Solar energy storage using phase change materials, *Renewable and Sustainable Energy Reviews* 11 (2007) 1913–1965.
4. Y. Hong, G. Xin-Shi, Preparation of polyethylene–paraffin compound as a form-stable solid-liquid phase change material, *Solar Energy Materials and Solar Cells* 64 (2000) 37–44.
5. F. Asinger, *Paraffins: Chemistry and Technology*. Pergamon Press, 1967.
6. RUBITHERM GmbH website.
7. H. Inaba, P. Tu, Evaluation of thermophysical characteristics on shape-stabilized paraffin as a solid-liquid phase change material, *Heat and Mass Transfer* 32 (1997) 307–312.
8. I. Krupa, G. Mikova, A.S. Luyt, Shape stabilized phase change materials based on low density polyethylene and paraffin waxes, *European Polymer Journal* 43 (2007) 4695–4705.
9. S. Kim, L.T. Drzal, High latent heat storage and high thermal conductive phase change materials using exfoliated graphite nanoplatelets, *Solar Energy Materials and Solar Cells* (3 (2009) 136–142.
10. J. Zhao, Y. Guo, F. Feng, Q. Tong, W. Qv, H. Wang, Microstructure and thermal properties of a paraffin/expanded graphite phase-change composite for thermal storage, *Renewable Energy* 36 (2011) 1339–1342.
11. J. Fukai, Y. Hamada, Y. Morozumi, O. Miyatake, Effect of carbon-fibre brushes on conductive heat transfer in phase change materials, *International Journal of Heat and Mass Transfer* 45 (2002) 4781–4792.
12. Y. Cui, C. Liu, S. Hu, X. Yu, The experimental exploration of carbon nanofiber and carbon nanotube additives on thermal behaviour of phase change materials, *Solar Energy Materials and Solar Cells* 95 (2011) 1208–1212.

13. J. Xiang, L.T. Drzal, Investigation of exfoliated graphite nanoplatelets (xGnP) in improving thermal conductivity of paraffin wax-based phase change material, *Solar Energy Materials and Solar Cells* 95 (2011) 1811-1818.
14. L. Xia, P. Zhang, R.Z. Wang, Preparation and thermal characterization of expanded graphite/paraffin composite phase change material, *Carbon* 48 (2010) 2538-2548.
15. J.A. Molefi, A.S. Luyt, I. Krupa, Comparison of the influence of Cu micro- and nano-particles on the thermal properties of polyethylene/Cu composites, *eXPRESS Polymer Letters* 3 (2009) 639-649.
16. J.A. Molefi, A.S. Luyt, I. Krupa, Comparison of the influence of copper micro- and nano-particles on the mechanical properties of polyethylene/copper composites, *Journal of Materials Science* 45 (2010) 82-88.
17. J.A. Molefi, A.S. Luyt, I. Krupa, Investigation of thermally conducting phase change materials based on polyethylene/wax blends filled with copper particles, *Journal of Applied Polymer Science* 116 (2010) 1766-1774.
18. A.S. Luyt, I. Krupa, Thermal behaviour of low and high molecular weight paraffin waxes used for designing phase change materials, *Thermochimica Acta* 467 (2008) 117-120.

DOI: 10.1016/j.tca.2007.11.001

Table 1 BET specific surface areas of graphite samples

Sample	Surface area (m² g⁻¹)
Expandable graphite ES 250 B5	2.40
Expanded ES 250 B5	16.30
Zimbabwean graphite	4.27

Table 2 Composite formulations

Sample	Graphite / wt. %	Wax / g	LDPE / g	Graphite / g
Wax/LDPE	0	450.00	300.00	0.00
	10	450.00	300.00	83.33
Zimbabwean graphite	15	450.00	300.00	132.35
	20	450.00	300.00	187.50
	25	450.00	300.00	250.00
	5	450.00	300.00	39.47
Expanded ES250 B5	7	450.00	300.00	56.45
	10	450.00	300.00	83.33

Table 3 Compounding temperature profile

Extruder zone	1	2	3	Die
Set temperatures / °C	130	140	150	150

Table 4 DSC data for the heating of the different samples after initially heating to 70 °C and cooling to 0 °C

Sample	$\Delta H_m / \text{J g}^{-1}$	$\Delta H^{\text{calc}} / \text{J g}^{-1}$	Peak / °C
wax	169.8		54.9
LDPE	84.1		108.9
60/40 w/w wax/LDPE	94.6	101.9	54.8
	40.5	33.6	97.0
95/5 w/w (wax/LDPE)/e-graphite	96.4	96.8	55.3
	37.4	32.0	95.8
93/7 w/w (wax/LDPE)/e-graphite	89.3	94.7	54.1
	33.1	31.3	95.6
90/10 w/w (wax/LDPE)/e-graphite	88.3	91.7	55.1
	33.5	30.3	97.8
90/10 w/w (wax/LDPE)/graphite	83.9	91.7	55.6
	36.2	30.3	94.3
85/15 w/w (wax/LDPE)/graphite	77.0	86.6	54.8
	34.7	28.6	95.9
80/20 w/w (wax/LDPE)/graphite	76.6	81.5	56.4
	29.2	26.9	96.4
75/25 w/w (wax/LDPE)/graphite	69.6	76.4	54.6
	31.7	25.2	94.7

Table 5 DSC data for the heating of the different samples after initially heating to 150 °C and cooling to 0 °C

Sample	$\Delta H / \text{J g}^{-1}$	$\Delta H^{\text{calc}} / \text{J g}^{-1}$	Peak / °C
wax	168.2		56.8
LDPE	72.7		109.1
60/40 w/w wax/LDPE	85.2	101.0	54.8
	15.9	29.1	98.1
95/5 w/w (wax/LDPE)/e-graphite	83.2	95.9	55.8
	14.9	27.6	98.7
93/7 w/w (wax/LDPE)/e-graphite	82.1	93.9	54.4
	15.2	27.0	97.6
90/10 w/w (wax/LDPE)/e-graphite	80.0	90.9	54.4
	14.3	26.2	97.8
90/10 w/w (wax/LDPE)/graphite	79.0	90.9	55.1
	17.9	26.2	97.6
85/15 w/w (wax/LDPE)/graphite	81.6	85.8	54.3
	16.9	24.7	97.6
80/10 w/w (wax/LDPE)/graphite	80.2	80.8	55.1
	15.9	23.3	97.0
75/25 w/w (wax/LDPE)/graphite	62.2	75.7	53.9
	10.1	21.8	97.6

Table 6 DMA storage modulus data for all the investigated samples

Sample	E' at -40 °C	E' at 70 °C
LDPE	$(2.43 \pm 0.01) \times 10^9$	$(1.18 \pm 0.00) \times 10^8$
60/40 w/w wax/LDPE	$(1.42 \pm 0.07) \times 10^9$	$(2.90 \pm 0.23) \times 10^7$
95/5 w/w (wax/LDPE)/e-graphite	$(1.63 \pm 0.21) \times 10^9$	$(4.09 \pm 0.27) \times 10^7$
93/7 w/w (wax/LDPE)/e-graphite	$(1.74 \pm 0.16) \times 10^9$	$(5.62 \pm 2.53) \times 10^7$
90/10 w/w (wax/LDPE)/e-graphite	$(1.64 \pm 0.14) \times 10^9$	$(7.33 \pm 0.82) \times 10^7$
90/10 w/w (wax/LDPE)/graphite	$(1.37 \pm 0.31) \times 10^9$	$(4.74 \pm 0.80) \times 10^7$
85/15 w/w (wax/LDPE)/graphite	$(1.67 \pm 0.39) \times 10^9$	$(5.56 \pm 1.03) \times 10^7$
80/20 w/w (wax/LDPE)/graphite	$(1.74 \pm 0.45) \times 10^9$	$(7.16 \pm 0.88) \times 10^7$
75/25 w/w (wax/LDPE)/graphite	$(2.01 \pm 0.06) \times 10^9$	$(7.33 \pm 1.28) \times 10^7$

Figure captions

- Figure 1 Graphite particle size distribution
- Figure 2 SEM micrographs of the graphites; A: Zimbabwean graphite, B: Expandable graphite ES250 B5, C: Expanded graphite ES250 B5, D: Expanded graphite ES250 B5 (high resolution)
- Figure 3 Thermal conductivities of LDPE/wax blends containing different amounts of graphite and e-graphite
- Figure 4 SEM micrographs of the surfaces of (a) 90/10 w/w (wax/LDPE)/graphite and (b) 90/10 w/w (wax/LDPE)/e-graphite
- Figure 5 TGA curves of LDPE/wax blends containing different amounts of (a) graphite and (b) e-graphite
- Figure 6 DSC heating curves of LDPE/wax blends containing different amounts of (a) graphite and (b) e-graphite, after initial heating to 70 °C and cooling to 0 °C
- Figure 7 DSC heating curves of LDPE/wax blends containing different amounts of (a) graphite and (b) e-graphite, after initial heating to 150 °C and cooling to 0 °C
- Figure 8 DSC isothermal melting curves at 45 °C for the LDPE/wax blend and two LDPE/wax/graphite composites containing different amounts of (a) graphite and (b) e-graphite
- Figure 9 DMA loss modulus curves of LDPE/wax blends containing different amounts of (a) graphite and (b) e-graphite

Figure 1

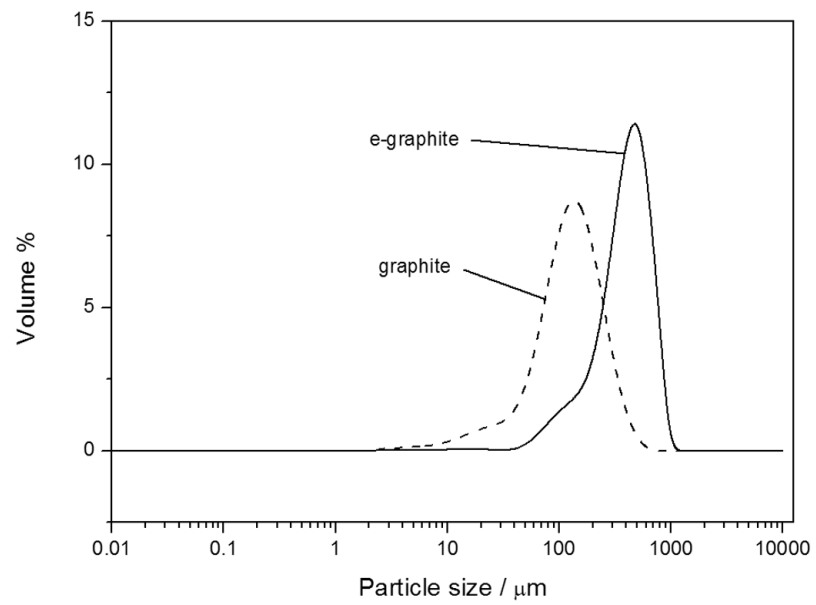


Figure 2

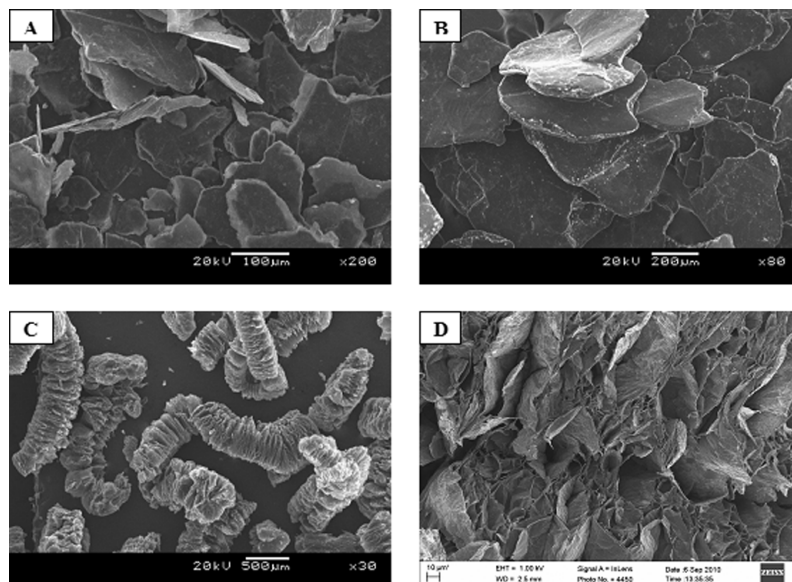


Figure 3

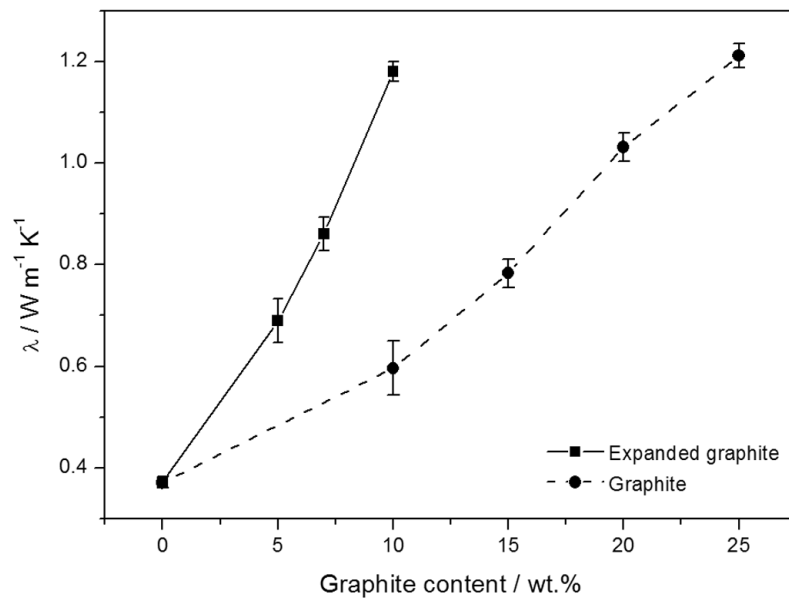


Figure 4

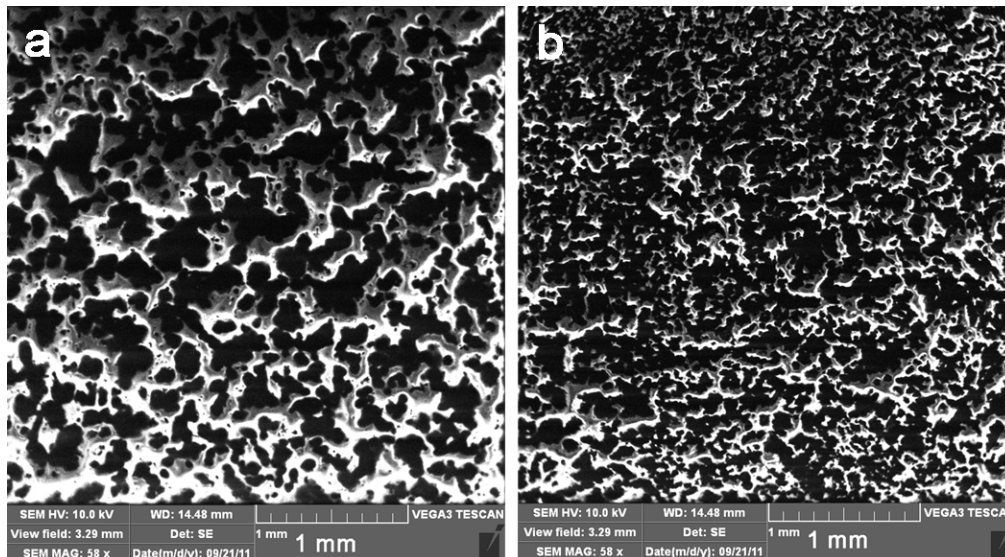


Figure 5

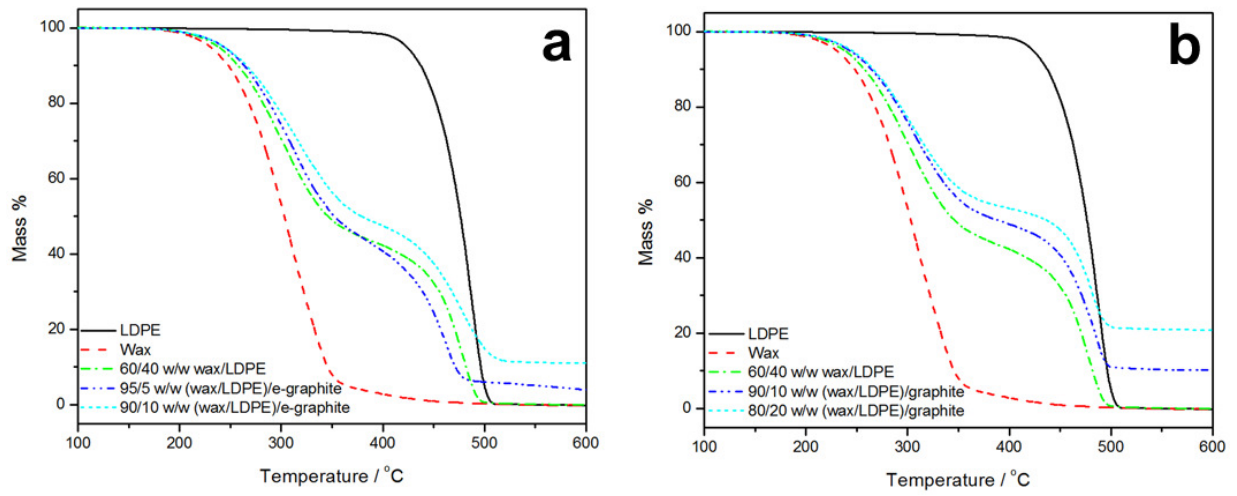


Figure 6

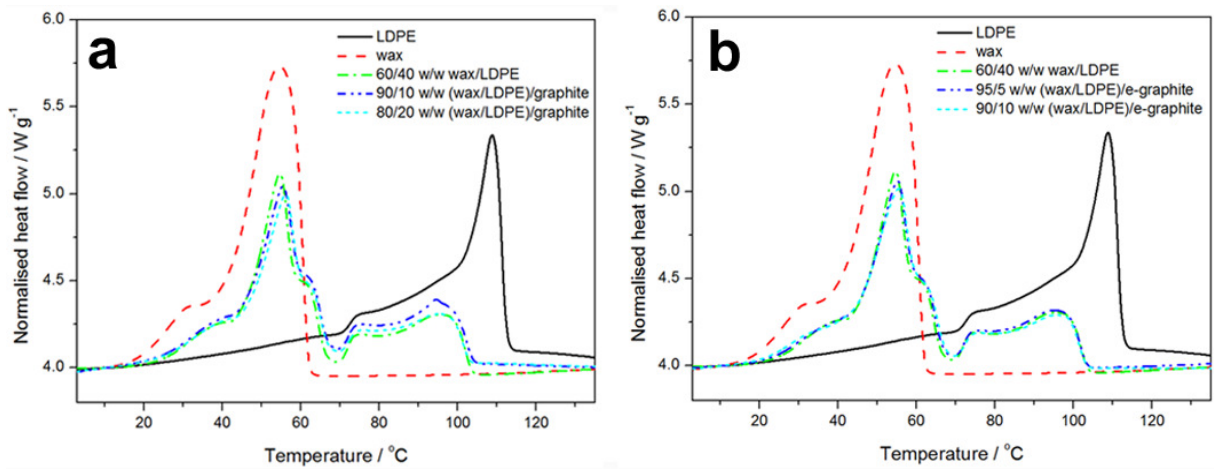


Figure 7

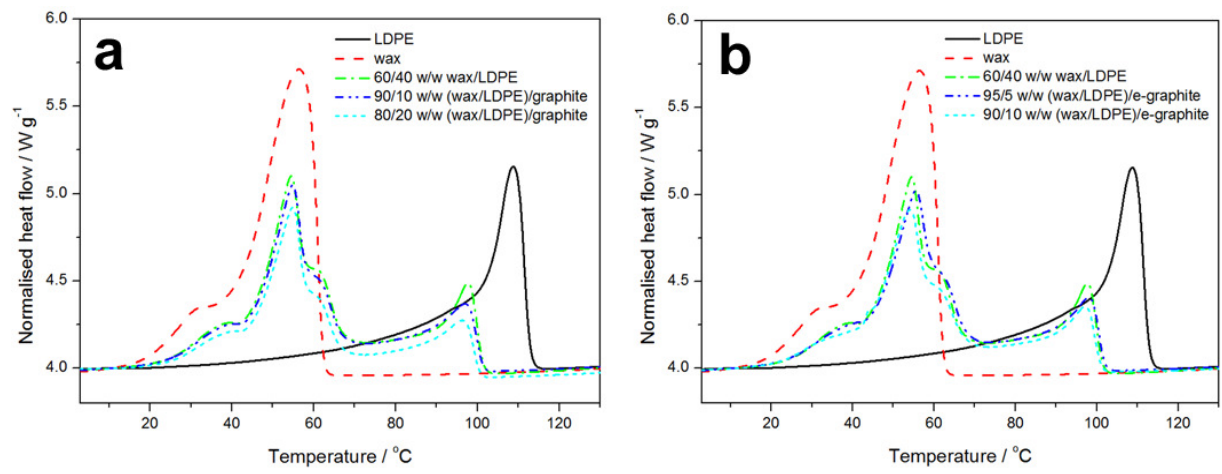


Figure 8

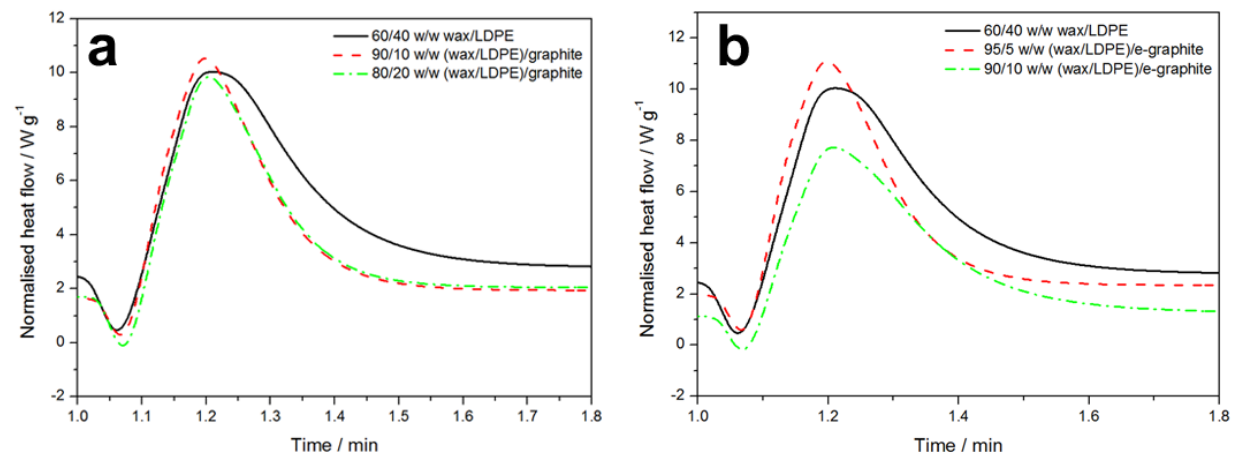


Figure 9

